Supporting Information

The Response of Charge Transfer Properties to Electric Fields in Organic Semiconductors: A Comprehensive Theoretical Investigation

Hengyue Zhang, [‡, a, b, c, d] Jie Zhu, [‡, a, b] Xinxin Niu,[a, b] Qian Zhang,[a, b] Yajing Sun,*[a, b] and Weigang Zhu*[a]

[a] *Key Laboratory of Organic Integrated Circuits, Ministry of Education & Tianjin Key Laboratory of Molecular Optoelectronic Sciences, Department of Chemistry, School of Science, Tianjin University, Tianjin 300072, China*

[b] *Haihe Lab of ITAI, Tianjin 300051, China*

[c] *School of Chemical Engineering and Technology, Tianjin University, Tianjin, 300354, PR China*

[d] *College of Chemistry, Nankai University, Tianjin, 300071, PR China*

*Corresponding author

‡ Equal Contributions

E-mail address: syj19@tju.edu.cn (Y. Sun), w_zhu10@tju.edu.cn (W. Zhu)

1. Geometry Structure

1.1 Molecular Packing Distances

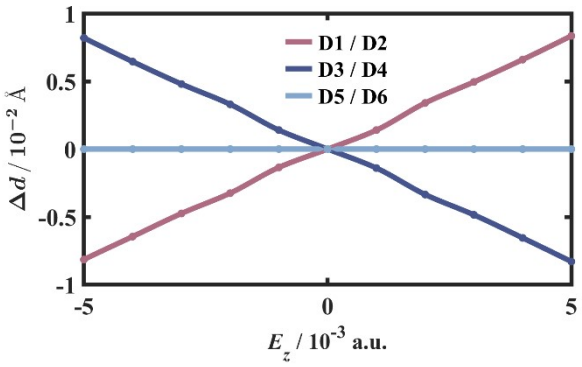

Figure S1 The distances variation between the two adjacent molecular in the dimers under the external electric field along z axis.

1.2 The Bond Angles

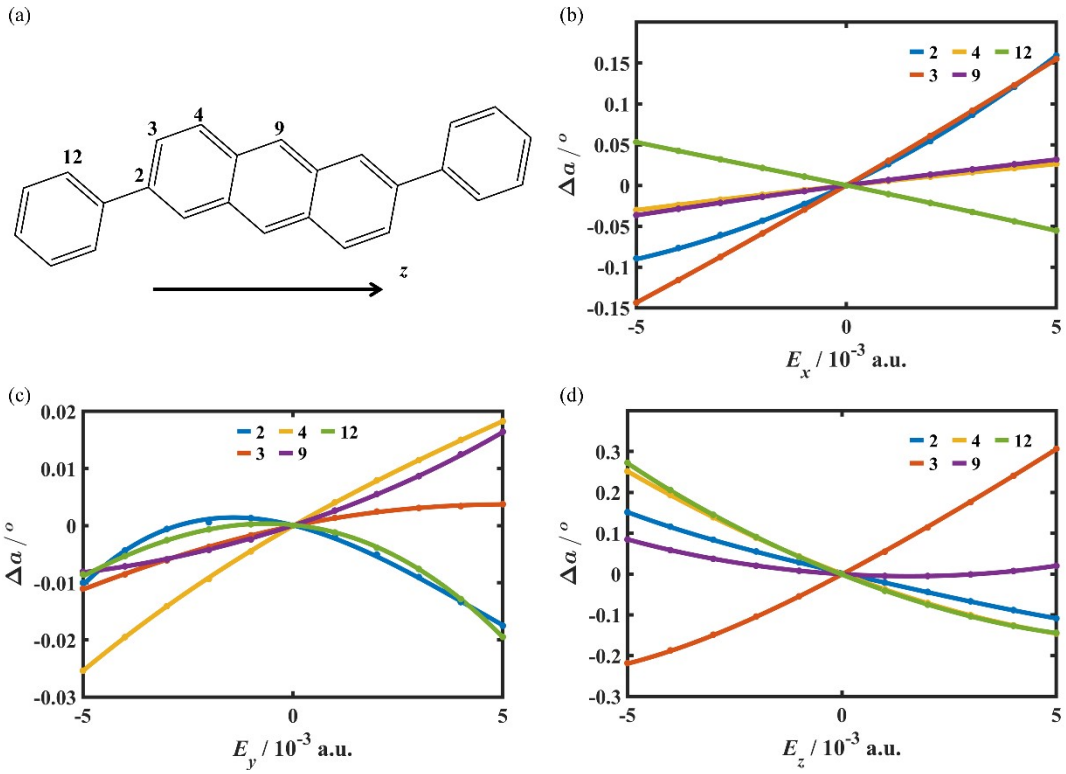

Fig S2 (a) Geometry structure of DPA, the numbers denote the vertex of the bond angles composed of carbon atoms within the aromatic ring. The bond angles variation induced by the electric fields along (b) x, (c) y and (d) z axis.

2. Charge Transport Properties

2.1 Carrier Mobility along z-axis

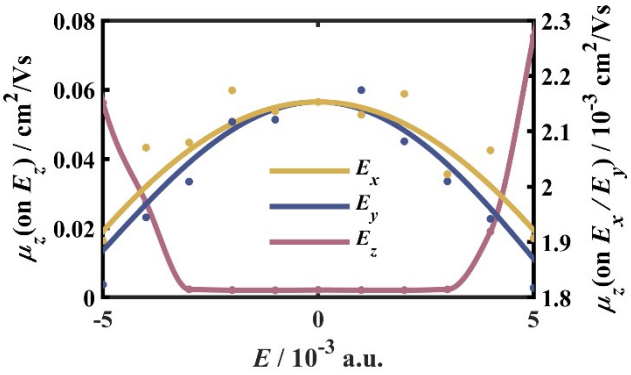

Fig S3 Carrier mobility along z axis with the external electric fields.

2.2 Normal Modes Analysis

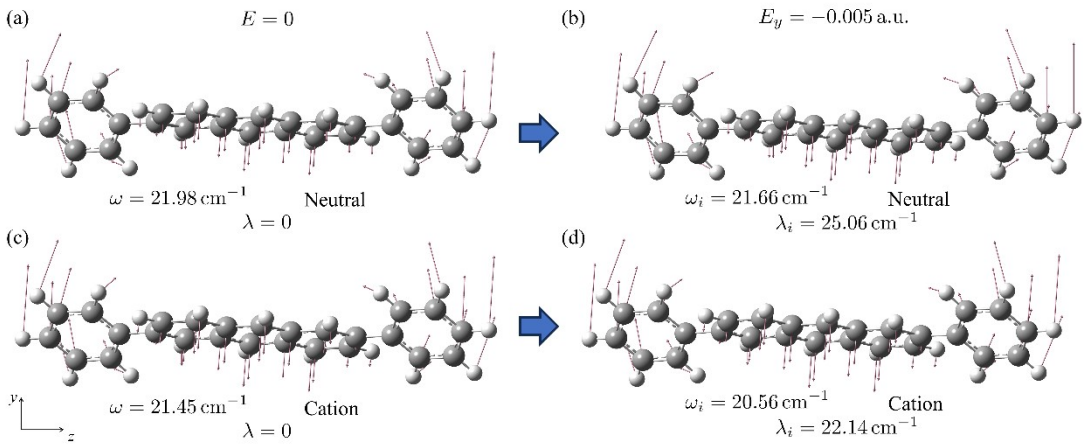

Figure S4 Two representative normal modes which contributes a lot to the increasement of reorganization energy and the change of their reorganization energy contributions when electric along y axis is applied.

2.3 Huang-Rhys factor

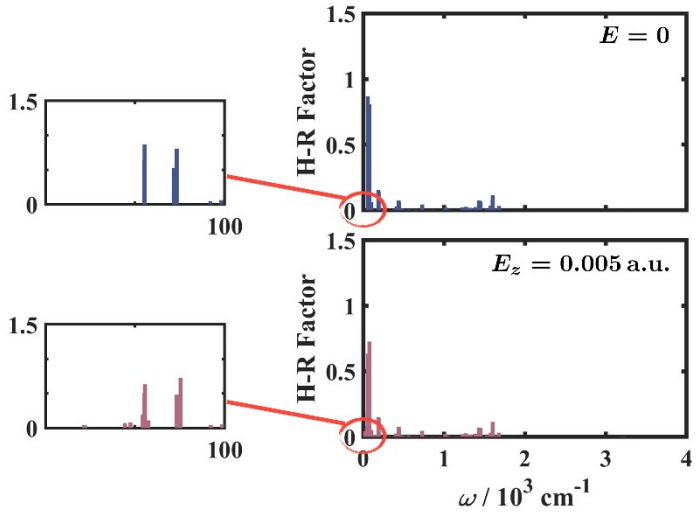

Figure S5 Huang-Rhys factor of each normal mode with and without electric fields along x axis applied.

2.4 Transfer Integrals s

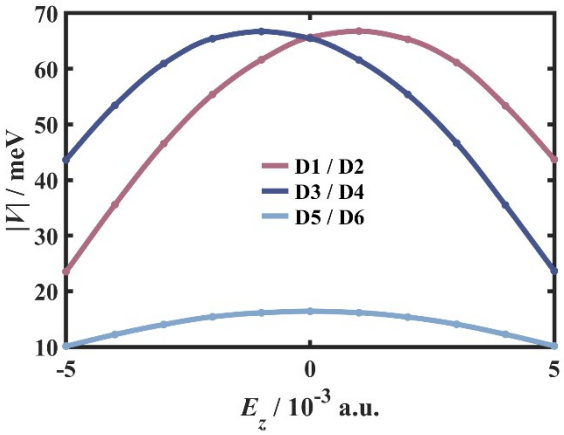

Figure S6 Transfer integral variation when electric field along z axis applied

3. Simulation in OFET

3.1 Simulation Method

The process of simulating the intrinsic carrier mobility in a working organic field effect transistor device consists of **four steps**.

Step1. Obtain initial data.

We have obtained the mobility under an electric field along the Cartesian axis. However, in real devices, the electric field is usually not oriented along the axis. Therefore, we need more data for the simulation. Here, we calculate the mobility under electric fields along different directions 0.001, 0.003 and 0.005 a.u. as a supplement. The calculations are the same as described in the Methods section.

Step2. Numerical Fitting.

Numerical fitting was performed using the least squares method. We fitted the mobility along the x-axis and y-axis separately. Take the mobility along the x-axis (denoted by μ_x) as an example. First, we fitted the relationship between the mobility and the electric field along the Cartesian axis. We used polynomial fits to express this relationship. These functions are denoted by $\mu_x^{'}(E)$, $\mu_y^{'}(E)$, and $\mu_z^{'}(E)$, respectively. It is encouraging to note that all the fits have high coefficients of determination (R^2) as shown in **Fig. S7**. We then performed the following fits using the carrier mobility in the off-axis electric field. Here, we construct a numerical model expressed as,

$$\mu_x = \sqrt[3]{\mu_x^{'}(E_x)\mu_y^{'}(E_y)\mu_z^{'}(E_z)} + aE_xE_y + bE_xE_z + cE_yE_z + d$$

Where, the projections of electric field *E* along Cartesian axis are denoted as E_x, E_y, and E_z, and *a*-*d* are fitted constants.

Step3. Obtaining the electric field distribution.

We use the Silvaco TCAD Atlas device simulation package to calculate the electric field distribution in an actual OFET. In the simulation, we chose pentacene as the substrate material for the organic semiconductor. To simplify the calculations, we consider the dielectric constant to be isotropic. The dielectric constant is set to 2.2822, which corresponds to the dielectric constant of DPA, and it is determined by the Clausius-Mossotti equation. The Clausius-Mossotti equation is[1],

$$\frac{\varepsilon_r - 1}{\varepsilon_r + 2} = \frac{\rho N_A \alpha}{3M\varepsilon_0}$$

Where, ε_r denotes the dielectric constant, ρ represents the density, *M* represents the molecular mass, N_A = 6.02 × 10^{23} mol^{-1} represents the Avogadro constant, ε_0 = 8.854 × 10^{-12} F/m represents the vacuum permittivity, and α denotes the electronic polarizability, which is calculated with Gaussian 09[2] Package at the level of PBE0/jul-cc-pVDZ. We set the voltage

between source and gate electrodes V_{GS} to be -40 V, and the voltage between source and drain electrodes V_{DS} to be -20 V to carry out this simulation.

Step4. Obtaining the mobility along the conducting channel.

Based on the above simulations, we extracted the electric field distribution on the conducting channel. By numerically fitting the model, we obtained the carrier mobility distribution along the channel.

3.2 The Numerical Fitting Process

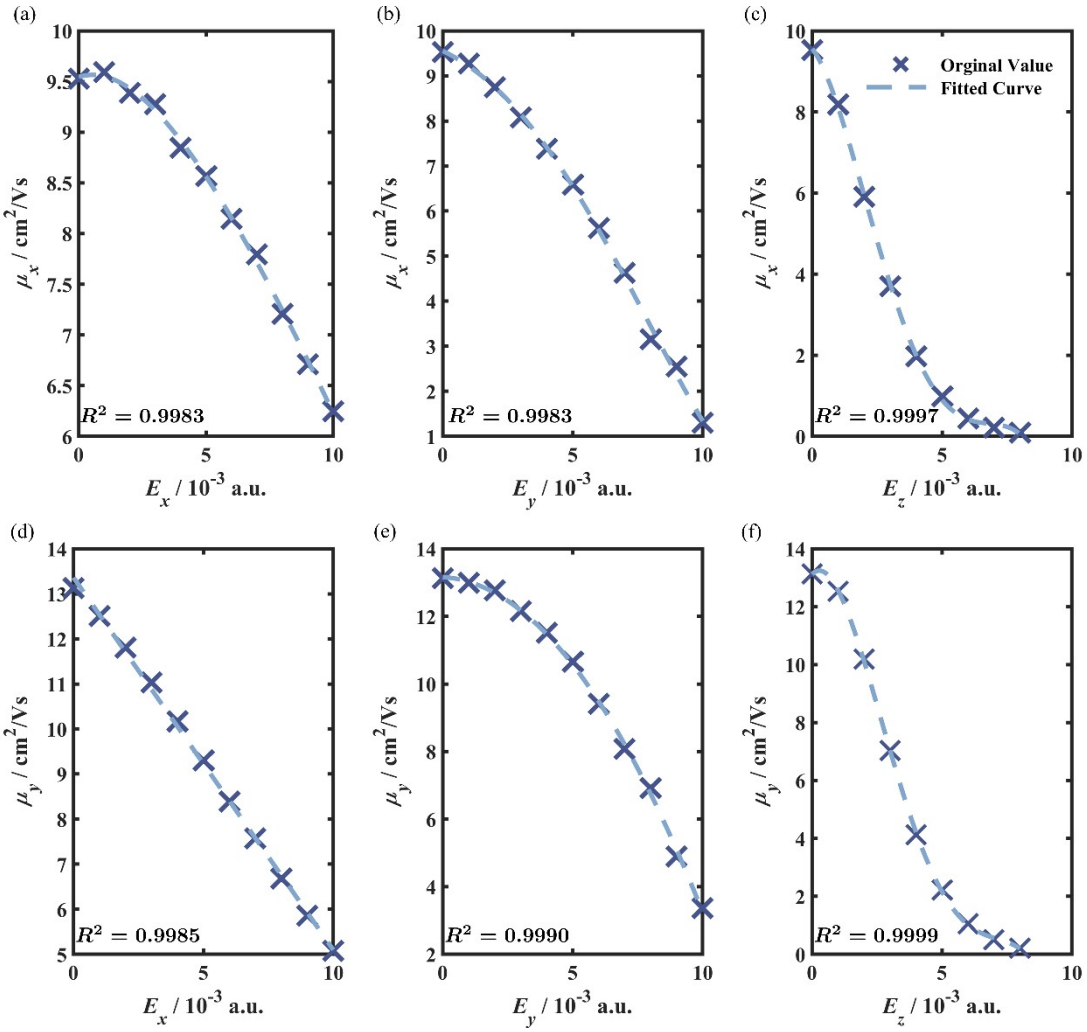

Figure S7 The fitting result of the mobility along x axis effected by electric directions along (a) x, (b) y, and (c) z directions and the mobility along y axis effected by electric directions along (d) x, (e) y, and (f) z directions.

3.3 The Fitting Results

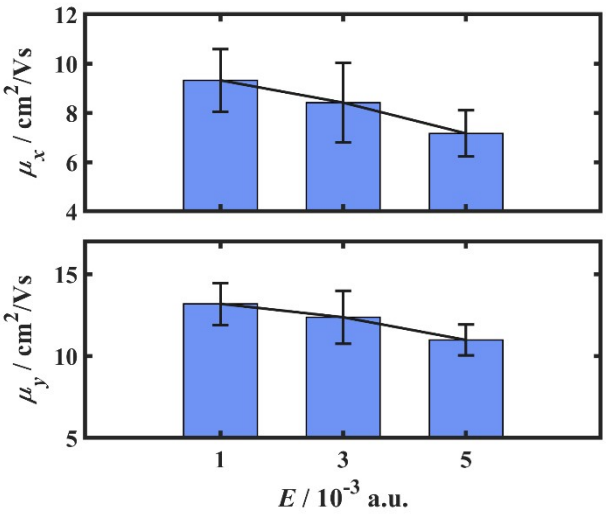

Figure S8 The mean result of the predicted mobility under different values of electric fields. The error bars represent the standard error.

4. References

1 L. Benatto and M. Koehler, *J. Phys. Chem. C*, 2019, **123**, 6395–6406.

2 M. J. Frisch, G. W. Trucks, H. B. Schlegel, G. E. Scuseria, M. A. Robb, J. R. Cheeseman, G. Scalmani, V. Barone, B. Mennucci, G. A. Petersson, H. Nakatsuji, M. Caricato, X. Li, H. P. Hratchian, A. F. Izmaylov, J. Bloino, G. Zheng, J. L. Sonnenberg, M. Hada, M. Ehara, K. Toyota, R. Fukuda, J. Hasegawa, M. Ishida, T. Nakajima, Y. Honda, O. Kitao, H. Nakai, T. Vreven, J. A. Montgomery Jr., J. E. Peralta, F. Ogliaro, M. Bearpark, J. J. Heyd, E. Brothers, K. N. Kudin, V. N. Staroverov, R. Kobayashi, J. Normand, K. Raghavachari, A. Rendell, J. C. Burant, S. S. Iyengar, J. Tomasi, M. Cossi, N. Rega, J. M. Millam, M. Klene, J. E. Knox, J. B. Cross, V. Bakken, C. Adamo, J. Jaramillo, R. Gomperts, R. E. Stratmann, O. Yazyev, A. J. Austin, R. Cammi, C. Pomelli, J. W. Ochterski, R. L. Martin, K. Morokuma, V. G. Zakrzewski, G. A. Voth, P. Salvador, J. J. Dannenberg, S. Dapprich, A. D. Daniels, Ö. Farkas, J. B. Foresman, J. V. Ortiz, J. Cioslowski and D. J. Fox, Gaussian∼09 Revision E.01 2016.